C_6Yb and graphite: A comparative high-pressure transport study

A. Akrap,[1] T. Weller,[2] M. Ellerby,[2] S. S. Saxena,[3] G. Csányi,[3] and L. Forró[1]
[1]*Institut de Physique de la matière complexe, EPFL, CH-1015 Lausanne, Switzerland*
[2]*Department of Physics and Astronomy, University College London, Gower Street, London WCIE 6BT, United Kingdom*
[3]*Cavendish Laboratory, University of Cambridge, Madingley Road, Cambridge CB3 0HE, United Kingdom*
(Received 28 November 2006; revised manuscript received 3 April 2007; published 26 July 2007)

We report the high-pressure behavior of the resistivity $\rho(T)$ and thermoelectric power $S(T)$ for both superconducting C_6Yb and its pristine material, highly oriented pyrolytic graphite (HOPG), in the pressure range up to 2.3 GPa. Whereas the pressure dependence of $\rho(T)$ is weak in HOPG, in C_6Yb there is a strong increase of the residual resistivity, which we attribute to the corrugation of the graphene sheets. The pressure behavior of T_c in C_6Yb correlates with the slope of resistivity, $\partial\rho/\partial T$, indicating a possible role of phonons in the superconductivity mechanism. Finally, $S(T)$ demands a two-band picture in HOPG while a single band provides a good description for C_6Yb.

DOI: 10.1103/PhysRevB.76.045426 PACS number(s): 74.70.−b, 74.25.Fy, 74.62.Fj

I. INTRODUCTION

Graphite has occupied a distinguished place in the field of condensed matter research, and this has been revived after the recent discovery of unusually high critical temperatures in graphite-derived C_6Ca and C_6Yb.[1,2] The layered honeycomb structure of pristine graphite in many aspects determines its physical properties, accounting for the quantum Hall effect,[3] Dirac dispersion of electrons,[4] and other curious phenomena. Apart from a very low charge density, graphene sheets are characterized by a high carrier mobility, which makes graphite an interesting matrix for the synthesis of intercalation compounds (GICs).[5,6] An order of magnitude increase in the superconducting transition temperatures of GICs was brought about by the synthesis of C_6Yb and C_6Ca,[1,2] where the transition temperatures are 6.5 K and 11.5 K, respectively. This discovery caused an upsurge of activity, focusing mainly on explaining the mechanism of superconductivity in these two systems.[7–10] In order to understand the high critical temperature, one has to know the detailed behavior of transport coefficients. The unusual behavior of the transport coefficients under high pressure provides a deeper insight into the mechanism of superconductivity in these compounds. To separate what is specific to the superconducting compound C_6Yb, one has to know the response of the pristine, nonintercalated material to the pressure. Although much theoretical and experimental work has been done on the electrical and thermal transport properties of graphite, there are open questions left arising from the high pressure behavior.

In this article, we report the resistivity and Seebeck effect for C_6Yb, both markedly different from those of the starting material—highly oriented pyrolytic graphite (HOPG). The resistivity shows typically metallic behavior with a quadratic term at low temperatures, characteristic of electron-electron correlations. The coefficient A describing the T^2 dependence increases with pressure. However, the strongest pressure dependence is observed for the residual resistivity. We explain its increase by the warping of the graphene sheets. The Seebeck coefficient or thermoelectric power (TEP) shows a clearly metallic temperature dependence. This suggests a single-band description, as opposed to graphite where a two-carrier description is needed due to the semimetallic character of the electronic structure.

II. MATERIALS AND METHODS

The samples of C_6Yb were prepared by doping HOPG with Yb. The same batch of HOPG was used to study the nonintercalated system. The good quality of C_6Yb samples is described by their residual resistivity ratio (RRR) of 25. In the case of HOPG samples, the RRR was 7, which is a typical value for this system.[11] All of the transport measurements were done in the direction of the graphene planes. The electrical resistivity and Seebeck effect were measured simultaneously in a purpose-built pressure cell, using silver paint as a means of contacting and a Chromel-Constantan thermocouple to determine the temperature gradient on the sample. Due to its air sensitivity, C_6Yb was handled and mounted in a glove box, under argon atmosphere. The pressure range was from 1 bar to 2.3 GPa. The applied hydrostatic pressure was monitored in the entire 4–300 K range with a calibrated InSb pressure gauge, and kerosene served as pressure-transmitting medium.

The band structure calculations were performed by a method which is described in Ref. 12.

III. RESULTS AND DISCUSSION

The ambient pressure in-plane resistivity of graphite, shown in Fig. 1(a), agrees with previous measurements.[11,13] The temperature dependence is almost linear at high temperatures and shows a more pronounced change below 100 K, ending in a T^2 temperature dependence at the lowest temperatures. The coefficient A, which describes the low temperature resistivity as

$$\rho(T) = \rho_0 + AT^2, \tag{1}$$

is usually ascribed to carrier-carrier scattering. It was believed[13] that the overall shape of the resistivity is determined by the thermal motion of the Fermi level due to increased layer-layer interactions. However, it is quite likely

 ©2007 The American Physical Society

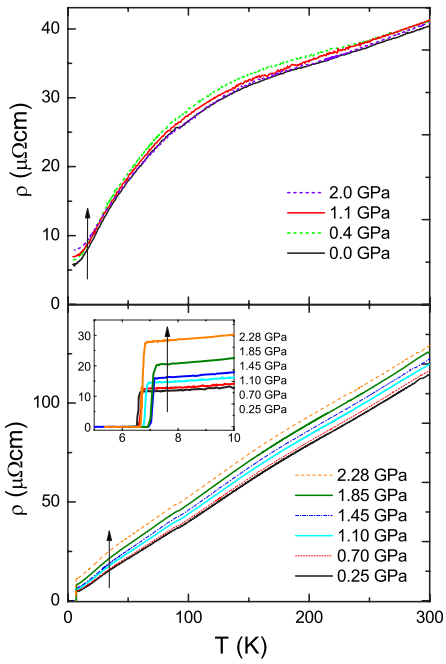

FIG. 1. (Color online) Resistivity of HOP graphite (above) and C_6Yb (below), under different pressures. The inset shows a blowup of the low-temperature resistivity in C_6Yb. The arrows indicate the direction in which pressure increases.

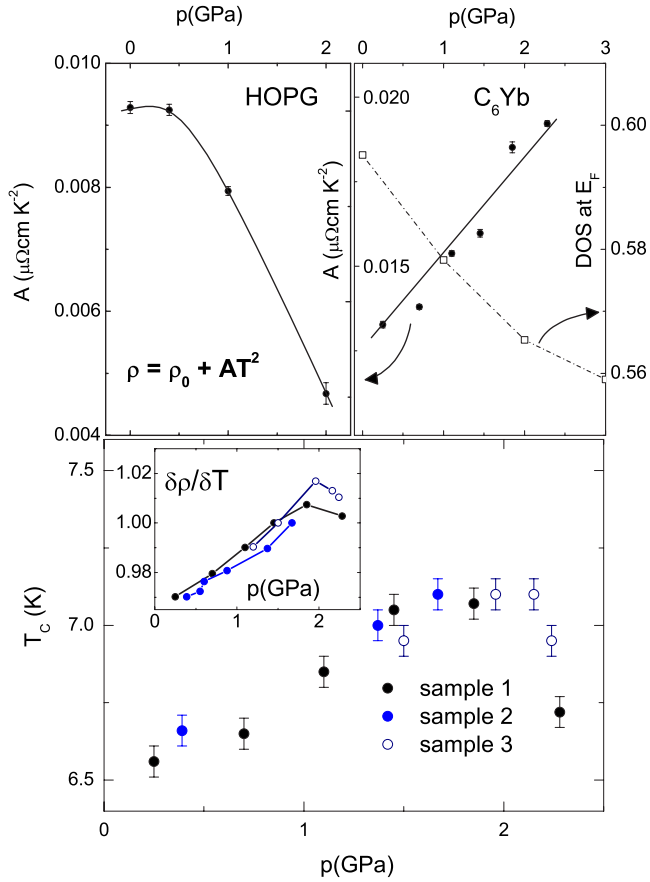

FIG. 2. (Color online) Upper panel, left: the pressure behavior of the coefficient A of the low-temperature T^2 resistivity in HOP graphite. Upper panel, right: the pressure dependence of A and of the DOS at the Fermi level in C_6Yb (right). Lower panel: Superconducting transition temperature for three samples of C_6Yb. Samples 1 and 2 have a RRR of 25, whereas for sample 3 the RRR is slightly lower at 23, due to air exposure. The initial linear increase in T_c of 0.4 K/GPa is followed by a saturation for $p > 1.8$ GPa and a decrease above 2.2 GPa. Inset: slope of the resistivity curves for C_6Yb, $\partial\rho/\partial T$, calculated from the data above 50 K, for the same three samples as in the lower panel. Values of the slope are normalized to 1 at 1.5 GPa. All connecting lines are guides for the eye.

that the pronounced decrease of resistivity below 100 K is influenced by the freezing out of the in-plane phonons.

The compressibility perpendicular to the graphene planes is very large: it is 30 times larger than in the planes.[5] Therefore, one would anticipate a strong pressure dependence of the Fermi level and a substantial increase of the carrier density available for transport. However, we see no significant pressure-influence on the in-plane resistivity, which implies that, although a partial compensation of the pressure effects on electrons and holes is possible, no major changes in the bandwidth take place.

The only features that do have an important pressure dependence in the pure graphite are the coefficient A from Eq. (1) and the residual resistivity ρ_0. An explanation for the decrease of A lies in the fact that as the planes get closer, the screening effect is enhanced and the electron-electron interaction weakens. The increase in ρ_0 under pressure probably has the same origin as in the Yb-intercalated system, which we will discuss below.

The ambient pressure resistivity of C_6Yb is substantially different from that of graphite. The room-temperature value of 115 $\mu\Omega$ cm is 2.5 times higher than in the pristine material, which implies a much stronger electron-phonon coupling. The temperature dependence of the resistivity is nearly linear, down to 15 K where the T^2 term appears. Pressure brings in three major changes. First, there is a strong increase of the residual resistivity in the whole temperature range. Second, there is an increase in the slope of resistivity in the quasilinear regime, $\partial\rho/\partial T$. Finally, the coefficient A increases (see Fig. 2).

Since the pressure-induced changes in the resistivity are all completely reversible, as we see upon releasing the pressure, we cannot attribute the increase in ρ_0 to the creation of microcracks in the sample. Similarly, we rule out the possibility of the reorganization of the Yb sublattice under pressure. According to recent calculations by one of the authors,[12] the structure of C_6Yb changes under high pressure. These calculations suggest that, in order to accommodate the large Yb atoms, the hexagons in the carbon sublattice deform into octagonal rings surrounded by pentagons. It is reasonable to expect the appearance of a warping of the graphene sheets under lower pressures, which appears within the background of intercalating Yb atoms and eventually leads to a structural transition. This warping would act as a static disorder and account for the observed temperature-independent increase in resistivity. Indeed, Gauzzi *et al.*[14] have observed signs of a pressure-induced transition in C_6Ca at 8 GPa, which they attribute to some form of structural transition or distortion, accompanied by a similar increase in residual re-

sistivity. This effect is also observed in pure graphite.[15] Although the pressure scale at which the calculations predict that a structural transition should take place, 18 GPa, is significantly above pressures we can currently reach experimentally, there is evidence that warped structures are energetically very close to the native structure between 2 and 18 GPa.[12]

In C_6Ca, there was an absence of T^2 behavior,[14] while we observe a clear T^2 dependence in C_6Yb with the coefficient A increasing with pressure. Such pressure dependence of A was not observed in graphite. This implies an enhancement of the effective electronic mass, but the band mass is expected to decrease under pressure, unless the effective electron-electron interaction strengthens. If this happens due to the enhanced coupling of electrons to phonons, then it may also be manifest in the T_c pressure dependence, shown in Fig. 2. Additionally, the slope of the nearly linear part of the $\rho(T)$ curve (inset in the lower panel of Fig. 2) is related to the strength of the electron-phonon coupling. We note that this slope $\partial\rho/\partial T$ increases with pressure, only to saturate above $\sim$1.8 GPa. This behavior is very similar to what is seen in the T_c pressure dependence, which may indicate a role of phonons for the superconductivity in this material. On the other hand, the pressure dependence of A and T_c may also be compatible with a scenario where acoustic plasmons are responsible for the superconductivity. Whereas it is hard to envisage a structural transition taking place at pressures as low as 2 GPa, it is possible that such a pressure is enough to push the interlayer band above the Fermi level. In that case, one would expect a sharp drop in T_c. Such a mechanism, based on screened acoustic plasmons, is theoretically possible in GICs[16] and might be realized in C_6Ca and C_6Yb.[17] However, in that case one would expect that the temperature dependence of the transport coefficients undergoes an important change when the interlayer band is pushed above the Fermi level, which we do not observe experimentally. Moreover, our band calculations do not show any significant shift of this band under pressure.

The thermoelectric power for graphite and C_6Yb under various pressures is shown in Fig. 3. This transport coefficient generally unravels fine features of the Fermi surface. Within Boltzmann transport theory, the part of TEP due to the diffusion of carriers can be calculated from the energy dependence of the conductivity, $\sigma(E)$, using Mott's formula:[18]

$$S_{Mott} = -\frac{\pi^2 k_B^2 T}{3e}\left(\frac{\partial \ln \sigma(E)}{\partial E}\right)_{E=E_F}. \quad (2)$$

TEP is the electronic transport property of a metal which is most sensitive to its Fermi energy.

The overall temperature dependence of thermopower in graphite at ambient pressure agrees well with the previous measurements by Morelli and Uher.[19] Because the thermopower crosses zero, a two-band model is needed to describe the transport in graphite. The total thermopower of a two-band conductor is given by a weighted sum of electronic and hole parts[20]:

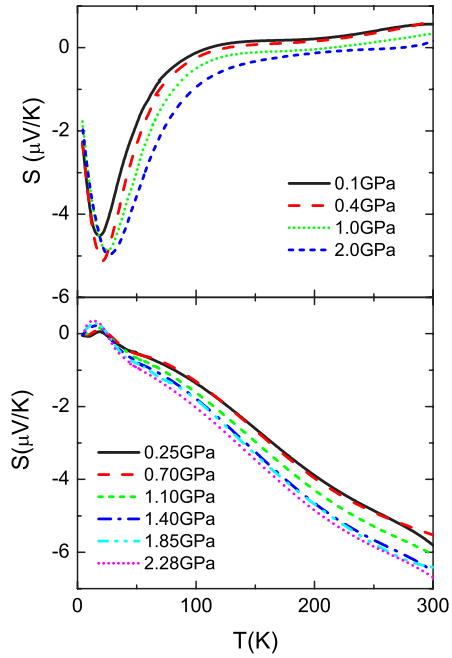

FIG. 3. (Color online) Thermoelectric power of graphite (top) and C_6Yb (bottom). The curves shown are polynomial interpolations of the data.

$$S_{Mott} = \frac{\sigma_e S_e + \sigma_h S_h}{\sigma_e + \sigma_h}. \quad (3)$$

From the ambient pressure TEP of graphite, one can see that in a broad temperature range the electrons and holes, with their respective mobilities, are compensated. This is consistent with tight-binding band structure calculations,[21] which assert that graphite behaves as a semiconductor with a vanishing energy gap, where in energy-momentum space the valence and conduction bands form circular cones around the Brilloiun zone edges.

Below 100 K, the same range which showed a fast decrease in ρ, the TEP of graphite rapidly changes, exhibiting a local minimum around 20 K, below which it tends toward zero. This peak is primarily a consequence of the phonon drag acting on both electrons and holes. However, we believe that the decrease in TEP below 100 K is enhanced, once again, due to the freezing out of phonon modes which limit the electronic mobility above 100 K. With pressure, the range of the temperatures where TEP decreases shifts to high temperatures. This is consistent with the idea that due to the increased elastic constants with pressure, the activation of the phonon modes happens at higher temperatures and consequently the change in carrier mobility starts at higher temperatures.[22]

With Yb intercalation the TEP becomes purely electron like, with a small absolute value of 6 μV/K at room temperature, typical of good metals like platinum (7 μV/K).[23] The temperature dependence is approximately linear down to 200 K. Using the classical electron transport formulas for the free electron gas, and assuming that there is a single, energy-independent relaxation time, we obtain[20]

$$S(T) = -\frac{\pi^2 k_B^2 T}{2|e|E_F}. \tag{4}$$

This equation allows us to extract the Fermi energy from the temperature slope of the TEP. Such an analysis gives a value of 2.0 eV at ambient pressure, which is in good agreement with the value from band structure calculations.[7] A change in slope around 100 K appears in the same range where we had a rapid TEP variation in the pristine graphite. Correspondingly, we attribute it to the in-plane phonon modes of graphene. If we understand the low-temperature peak as an effect of the phonon drag, it is visibly suppressed in comparison with pure graphite. This may be because the Yb intercalation produces disorder in the material, which shortens the mean free path of the phonons.

On top of the conventional metallic behavior of the Seebeck effect in C_6Yb, superimposed is its unconventional pressure dependence. In most metals, TEP decreases with pressure.[23] In C_6Yb, counterintuitively, both the slope and the absolute TEP value increase. If we analyze the data in the framework of Mott's formula with conductivity given in terms of Fermi-surface parameters,

$$\sigma = \frac{e^2}{12\pi^3\hbar}\tau(E_F)v_F S_F, \tag{5}$$

then the TEP is given by[24]

$$S = \frac{\pi^2 k_B^2 T}{3e}\left[\frac{d\ln N}{dE} + \frac{d\ln v^2}{dE} + \frac{d\ln \tau}{dE}\right]_{E=E_F}, \tag{6}$$

with τ, v, S_F, and N being the lifetime of electrons, velocity, Fermi surface area, and density of states (DOS), respectively. All these parameters, along with E_F, can change under pressure. According to our calculations of band structure, the DOS decreases under pressure, as shown in Fig. 2. Under 2 GPa, the DOS at the Fermi level is reduced by 5%. Furthermore, the calculations show that E_F increases by 0.14 eV under 2 GPa. Presumably, $\frac{dN}{dE}$ is not influenced as much as N. Therefore, the first term in Eq. (6), which is proportional to $\frac{1}{N}\frac{dN}{dE}|_{E_F}$, accounts for a part of the increase in the TEP. We have no clear indication how the Fermi surface velocity v_F changes under pressure, but we do see from the pressure dependence of resistivity that the scattering changes. However, what we see in the resistivity slope is less than a 5% change per 2 GPa, compared to an almost 20% increase in TEP in the same pressure range (Fig. 2). An alternative way to understand the increase of the absolute value of transport coefficients under pressure is to draw a comparison with the pure Yb system. There, both the TEP and resistivity are enhanced up to 4 GPa.[25,26] This anomaly was attributed to the pressure-induced decrease of the overlap between 6*s* and 6*p* bands.

From the TEP we can also infer some finer details. As in the undoped system, although less visible, there is a change in slope around 100 K, which gets smoother under pressure. Again, we attribute this to the freezing out of the breathing-mode phonons in carbon hexagons.

IV. CONCLUSION

The crucial point for grasping the physics of superconductivity in C_6Yb is to understand the pressure evolution of the superconducting transition temperature. In C_6Ca, the linear increase of T_c (Refs. 14, 17, and 27) and a quadratic behavior of the residual resistivity were observed up to 7 GPa. At that pressure, there is a sudden drop in T_c and, coincidentally, an abrupt change in ρ_0, both suggestive of a structural transition. In our case, $\rho_0 \propto p^2$ in the whole pressure range (not shown). Despite the fact that the DOS decreases with pressure, which is seen both from the band structure calculations and the evolution of TEP, the T_c increases. After the initial linear dependence on pressure, above 2.2 GPa the T_c decreases. This may be due to the increased electron-phonon interaction, which could be monitored as a change in slope of the nearly linear part of ρ. For all three samples we measured, this slope qualitatively follows the changes in T_c, which implies a possible role of phonons in the superconductivity of C_6Yb. Still, apart from phonons, pairing intermediated by acoustic plasmons remains a valid option. A plausible possibility is that pressures above 2 GPa shift the interlayer band above the Fermi energy, which would lead to a sudden drop in T_c.

In conclusion, we have performed a comparative high-pressure study of C_6Yb and its parent compound HOPG. In graphite, we noted a weak pressure dependence of the resistivity, corresponding to a decrease in the effective electron-electron interaction. We attributed this to the fact that the screening is enhanced as the pressure brings the graphene sheets nearer. In C_6Yb, we observed a strong increase of the residual resistivity, which may be understood in terms of a warping of the graphene sheets which would eventually, under much higher pressures, cause a structural instability. The thermoelectric power of graphite clearly demands a two-band picture, whereas C_6Yb is well described by a single electronic band. However, the pressure dependence of thermopower indicates that the band structure of C_6Yb could change in a nontrivial way under pressure.

It is a pleasure to acknowledge helpful discussions with Titusz Fehér and Neven Barišić. Part of the research was supported by the EPSRC-U.K. The work in Lausanne was sponsored by the Swiss National Science Foundation through the NCCR pool MaNEP. A.A. also acknowledges financial support by COST P16.

[1] T. E. Weller, M. Ellerby, S. S. Saxena, R. P. Smith, and N. T. Skipper, Nat. Phys. **1**, 39 (2005).
[2] N. Emery, C. Hérold, M. d'Astuto, V. Garcia, Ch. Bellin, J. F. Marêché, P. Lagrange, and G. Loupias, Phys. Rev. Lett. **95**, 087003 (2005).
[3] Y. Kopelevich, J. H. S. Torres, R. R. da Silva, F. Mrowka, H.

Kempa, and P. Esquinazi, Phys. Rev. Lett. **90**, 156402 (2003).
[4] K. S. Novoselov, A. K. Geim, S. V. Morozov, D. Jiang, M. I. Katsnelson, I. V. Grigorieva, S. V. Dubonos, and A. A. Firsov, Nature (London) **438**, 197 (2005).
[5] M. S. Dresselhaus and G. Dresselhaus, Adv. Phys. **30**, 139 (1981).
[6] R. Clarke and C. Uher, Adv. Phys. **33**, 469 (1984).
[7] G. Csányi, P. B. Littlewood, A. H. Nevidomskyy, C. J. Pickard, and B. D. Simons, Nat. Phys. **1**, 42 (2005).
[8] I. I. Mazin and S. L. Molodtsov, Phys. Rev. B **72**, 172504 (2005).
[9] I. I. Mazin, Phys. Rev. Lett. **95**, 227001 (2005).
[10] M. Calandra and F. Mauri, Phys. Rev. Lett. **95**, 237002 (2005).
[11] D. T. Morelli and C. Uher, Phys. Rev. B **30**, 1080 (1984).
[12] G. Csányi, C. J. Pickard, B. D. Simons, and R. J. Needs, Phys. Rev. B **75**, 085432 (2007).
[13] Y. Hishiyama and Y. Kaburagi, Carbon **30**, 483 (1992).
[14] A. Gauzzi, S. Takashima, N. Takeshita, C. Terkura, H. Takagi, N. Emery, C. Hérold, P. Lagrange, and G. Loupias, Phys. Rev. Lett. **98**, 067002 (2007).
[15] See, for example, W. L. Mao, H.-k. Mao, P. J. Eng, T. P. Trainor, M. Newville, C.-c. Kao, D. L. Heinz, J. Shu, Y. Meng, and R. J. Hemley, Science **302**, 425 (2003).
[16] B. Uchoa and A. H. Castro Neto, Phys. Rev. Lett. **98**, 146801 (2007).
[17] R. P. Smith, A. Kusmartseva, Y. T. C. Ko, S. S. Saxena, A. Akrap, L. Forró, M. Laad, T. E. Weller, M. Ellerby, and N. T. Skipper, Phys. Rev. B **74**, 024505 (2006).
[18] N. F. Mott, Proc. R. Soc. London, Ser. A **156**, 368 (1936).
[19] D. T. Morelli and C. Uher, Phys. Rev. B **31**, 6721 (1985).
[20] R. D. Barnard, *Thermoelectricity in Metals and Alloys* (Taylor & Francis, London, 1972).
[21] P. R. Wallace, Phys. Rev. **71**, 622 (1947).
[22] N. Barišić, R. Gaal, I. Kezsmarki, G. Mihály, and L. Forró, Phys. Rev. B **65**, 241403(R) (2002).
[23] J.-S. Zhou and J. B. Goodenough, Phys. Rev. B **54**, 13393 (1996).
[24] J. M. Ziman, *Electrons and Phonons* (Oxford University Press, New York, 1960).
[25] P. C. Souers and G. Jura, Science **140**, 481 (1963).
[26] N. V. Chandra Shekar, J. F. Meng, D. A. Polvani, and J. V. Badding, Solid State Commun. **116**, 443 (2000).
[27] J. S. Kim, L. Boeri, R. K. Kremer, and F. S. Razavi, Phys. Rev. B **74**, 214513 (2006).